IOPscience iopscience.iop.org

Home Search Collections Journals About Contact us My IOPscience

Three-body interactions in the condensed phases of helium atom systems

This article has been downloaded from IOPscience. Please scroll down to see the full text article.

2007 J. Phys.: Condens. Matter 19 116212

(http://iopscience.iop.org/0953-8984/19/11/116212)

View the table of contents for this issue, or go to the journal homepage for more

Download details:
IP Address: 129.252.86.83
The article was downloaded on 28/05/2010 at 16:36

Please note that terms and conditions apply.

IOP PUBLISHING JOURNAL OF PHYSICS: CONDENSED MATTER

J. Phys.: Condens. Matter **19** (2007) 116212 (16pp) doi:10.1088/0953-8984/19/11/116212

# Three-body interactions in the condensed phases of helium atom systems

**Sebastian Ujevic**[1] **and S A Vitiello**[2]

[1] CIFMC, Universidade de Brasília, 70904-970, Brasília—DF, Brazil
[2] Instituto de Física *Gleb Wataghin*, Universidade Estadual de Campinas, 13083 Campinas—SP, Brazil

E-mail: sujevic@unb.br and vitiello@ifi.unicamp.br

Received 19 October 2006, in final form 21 January 2007
Published 5 March 2007
Online at stacks.iop.org/JPhysCM/19/116212

**Abstract**

In this work we investigate how the description of several properties of helium atoms in the condensed phases are affected by the three-body terms of a very accurate inter-atomic potential. We introduce two phenomenological parameters in the three-body part of the inter-atomic potential in order to describe properly the equations of state of the solid and liquid phases. The calculations were performed using the multi-weight extension to the diffusion Monte Carlo method which allows accurate calculations of small energy differences in a significant way. The results show how the equations of state for both the liquid and solid phases and properties like the isothermal compressibility, the equilibrium, melting and freezing densities are affected by three-body interactions.

## 1. Introduction

The properties of helium systems at low temperature have attracted continuous experimental and theoretical interest. Several reviews have scrutinized the subject; for a recent one, see [1]. A basic aspect of the theoretical investigation of these systems is the inter-atomic potential used in the calculations. Recently [2] we put together a potential that is able to describe with great accuracy the equations of state for both the liquid and solid phases. It has two- and three-body components. The two-body part is the retarded potential published by Janzen and Aziz [3]. The three-body interaction includes the Axilrod–Teller–Muto (ATM) [4, 5] triple–dipole term and an exchange part as proposed by Cohen and Murrell [6].

In this work we investigate how the three-body interactions of our inter-atomic potential affect the description of several properties of the liquid and solid phases of $^4$He atoms. We want to gain a better understanding of the role played by the individual contributions of the three-body interactions. This is not only important by itself but also, for instance, as a means of

 © 2007 IOP Publishing Ltd Printed in the UK 

enhancing the physical content of the analytical functional forms that one might use to fit their contributions.

Some of the quantities in which we are interested are computed by taking energy differences that have quite similar magnitudes. The straightforward use of quantum Monte Carlo methods to compute such small energy differences might not be possible. The results of independent runs and their associated statistical uncertainties might render such calculations meaningless. To avoid such difficulties we use the multi-weight (MW) extension to the diffusion Monte Carlo (DMC) method [7, 8], which allows the calculation of small energy differences with great accuracy.

This work is organized as follows. In the next section we show the inter-atomic potential [2] used in the calculations. In section 3 we give an overview of how to use the MW extension of the DMC method to compute the three-body contributions to the total energy of a system of $^4$He atoms. Details of the numerical simulations are given in section 4. In the subsequent section we present our results and show how the three-body contributions of the inter-atomic potential affect the properties of the system. Section 6 contains some final comments. In the appendices we have reproduced from the literature the parameters of the two-body term and of the exchange three-body part of the potential used in this work.

## 2. Theory

The careful description of a system of helium atoms in condensed phases requires a Hamiltonian,

$$H_V = -\frac{\hbar^2}{2m}\sum_{i=1}^{N}\nabla^2_{\mathbf{r_i}} + V(R), \tag{1}$$

where the inter-atomic potential $V(R)$ [2] includes two- and three-body terms, and $R = \{\mathbf{r}_1, \mathbf{r}_2, \ldots, \mathbf{r}_N\}$ stands for the $N$ atoms' coordinates considered in the calculations. Its two-body part consists of the *ab initio* potential proposed by Korona *et al* [9], where retardation effects were included [3] through a function $\phi_{\mathcal{R}}$ in the dipole–dipole term

$$V_2(r) = A\exp(-\alpha r + \beta r^2) - f_6(r,\delta)\frac{C_6\phi_{\mathcal{R}}(r)}{r^6} - \sum_{n=4}^{8} f_{2n}(r,\delta)\frac{C_{2n}}{r^{2n}}, \tag{2}$$

where $A, \alpha, \beta, \delta, C_{2n}$ are parameters that have values reproduced in table A.1 of appendix A and the $f_{2n}$ are damping functions of the Tang–Toennies form [10]:

$$f_i(r,\chi) = 1 - \left(\sum_{k=0}^{i}(\chi r)^k/k!\right)\exp(-\chi r). \tag{3}$$

The retardation function $\phi_{\mathcal{R}}$ (see tables A.2 and A.3 in appendix A) smoothly changes the behaviour of the dipole–dipole dispersion term in the intermediate- and long-range region, slightly reducing the potential width.

The dispersion three-body contribution to the inter-atomic potential comes from the multipolar expansion of the third-order long-range polarization interaction of spherically symmetric atoms. We use a damped triple–dipole $ddd$ interaction term

$$V_{ddd}(\mathbf{r}_i,\mathbf{r}_j,\mathbf{r}_k) = C_9\frac{r_{ij}^2 r_{ik}^2 r_{jk}^2 + 3(\mathbf{r}_{ij}\cdot\mathbf{r}_{ik})(\mathbf{r}_{ji}\cdot\mathbf{r}_{jk})(\mathbf{r}_{ki}\cdot\mathbf{r}_{kj})}{r_{ij}^5 r_{ik}^5 r_{jk}^5} \times f_3(r_{ij},\delta_d) f_3(r_{ik},\delta_d) f_3(r_{jk},\delta_d), \tag{4}$$

where the $r_{ij} = |\mathbf{r}_{ij}|$ are the sides of the triangles formed by the atoms; $C_9 = 1.47$ (au) is the non-additive coefficient. By its very nature, the ATM interaction is not valid at short-range

distances. At this distance range, a reasonable description of the system requires this interaction to be damped. We have imposed this damping by a product of three Tang–Toennies $f_3(r, \delta_d)$ functions with $\delta_d = 20.352\ \text{nm}^{-1}$. The potential $V_{ddd}$ is positive for equilateral triangles and attractive for linear arrangements of atoms. The origin of this term is not difficult to understand. The dispersion energy due to dipole–dipole interaction arises from fluctuations in their atomic electronic cloud. A three-body component of this interaction will appear because, when an atom is put together with a pair, each dipole moment of this pair will respond to the dipole moment of the third atom.

For simplicity, we follow [11] and assume that the many-body dipole-interaction terms of fourth- and higher-order perturbation theory are cancelled by those of higher multipole third-order terms $ddq, qqd, ddo$ and $qqq$; $q$ stands for quadrupole and $o$ for octupole. On the other hand, the exchange correlation effects are supposed to be of importance, since for the helium trimers the non-additivity is probably dominated by the exchange forces.

In fact, the exchange interaction is needed in the inter-atomic potential and therefore we have used the analytical representation of Cohen and Murrell [6]:

$$\begin{aligned} V_J(\mathbf{r}_i, \mathbf{r}_j, \mathbf{r}_k) = \mathcal{A}[&c_0 + c_1 Q_{1(ijk)} + c_2 Q_{1(ijk)}^2 \\ &+ (c_3 + c_4 Q_{1(ijk)} + c_5 Q_{1(ijk)}^2)(Q_{2(ijk)}^2 + Q_{3(ijk)}^2) \\ &+ (c_6 + c_7 Q_{1(ijk)} + c_8 Q_{1(ijk)}^2)(Q_{3(ijk)}^3 - 3 Q_{3(ijk)} Q_{2(ijk)}^2) \\ &+ (c_9 + c_{10} Q_{1(ijk)} + c_{11} Q_{1(ijk)}^2)(Q_{2(ijk)}^2 + Q_{3(ijk)}^2)^2 \\ &+ (c_{12} + c_{13} Q_{1(ijk)} + c_{14} Q_{1(ijk)}^2)(Q_{2(ijk)}^2 + Q_{3(ijk)}^2) \\ &\times (Q_{3(ijk)}^3 - 3 Q_{3(ijk)} Q_{2(ijk)}^2)] \exp(-\alpha Q_{1(ijk)}) \end{aligned} \tag{5}$$

where we have introduced a fitted amplitude $\mathcal{A}$ that we have determined to be equal to 4.0. The $Q_1$, $Q_2$ and $Q_3$ are symmetry-adapted coordinates that depend on the triangle sides $r_{ij}$ and are given by

$$\begin{aligned} Q_{1(ijk)} &= \frac{1}{\sqrt{3}}(r_{ij} + r_{ik} + r_{jk}), \\ Q_{2(ijk)} &= \frac{1}{\sqrt{2}}(r_{ik} - r_{jk}), \\ Q_{3(ijk)} &= \frac{1}{\sqrt{6}}(2r_{ij} - r_{ik} - r_{jk}). \end{aligned} \tag{6}$$

The values of the parameters $\alpha$ and $\{c_i \mid i = 1, \ldots, 14\}$ determined by Cohen and Murrell are reproduced in table B.1 in appendix B.

The only two parameters that we have introduced [2] in the inter-atomic potential $V(R)$ is the amplitude $\mathcal{A}$ of (5) and the damping parameter $\delta_d$ of the Tang–Toennies function $f_3(r, \delta_d)$ of (3) used in the ATM term (4). These parameters were obtained through iterative least-squares fits. Several hundred configurations of independent runs with 108 particles at different densities of the liquid and solid phases were employed to fit the energies to the experimental values. For a matter of technical convenience, the fits were done by imposing a face-centred cubic (fcc) crystalline structure in the simulation of the solid phase. These calculations were performed with the inter-atomic potential $V(R)$. About 3000 configurations were used each time an iteration was performed. Once values of the amplitude $\mathcal{A}$ and the repulsive short-range $\delta_d$ were obtained, fresh configurations were generated for the next interaction. We continued this procedure until the energies converged.

## 3. The method

In order to learn how the three-body interactions $V_{ddd}$ and $V_J$ affect the description of systems of helium atoms, we have computed their contribution to the total energy. In our calculations we have applied the MW extension of the DMC method [7] to compute simultaneously the binding energies per atom for the Hamiltonians: $H_2$, where only the two-body potential of (2) is used; $H_{2ddd}$ determined by the potential $V_{2ddd} = V_2 + V_{ddd}$, the sum of $V_2$ and the triple–dipole interaction $V_{ddd}$ of (4); and $H_V$, which takes into account the full inter-atomic potential of (1) given by $V = V_2 + V_{ddd} + V_J$. This also includes the exchange term of (5). The contributions of $V_{ddd}$ and $V_J$ were computed by subtracting the appropriate correlated energies obtained with these Hamiltonians. In the following we give an overview of how the calculations are implemented.

In the MWDMC method, to each walker we associate more than one weight—one for each Hamiltonian of interest—and slightly generalize the usual DMC branching rules. The standard DMC method is accomplished by considering the following steps: diffusion, weight update and branching. As in the DMC method, in its MW extension the diffusion step depends only on a guiding function $\Psi_G$, which helps in the exploration of the important regions of the configuration space. The diffusion of a given set of walkers does not depend on any interacting potential of the system. So this step is performed exactly in the same way as in the standard DMC method. The simulations start with a given initial set of configurations or walkers with all weights set to one.

The diffusion of a walker from configuration $R'$ to a new one $R$ is performed by sampling

$$G_d(R, R') = (4\pi D\Delta\tau)^{-\frac{3N}{2}} \exp\left[-\frac{(R - R' - D\Delta\tau v_D(R'))^2}{4D\Delta\tau}\right], \tag{7}$$

where $v_D = 2\nabla \ln \Psi_G$ is the drift force, $D = \hbar^2/2m$ is the diffusion coefficient, and $\Delta\tau$ is the time step. To make our results as unbiased as possible, we have considered a time step like those of [12] and [13]. We have also imposed detailed balance condition.

After the diffusion, the weights $w'^{(k)}$ of a walker are updated according to

$$w^{(k)} = w'^{(k)} G_b^{(k)}(R, R'), \tag{8}$$

where the $G_b^{(k)}(R, R')$ are given by

$$G_b^{(k)}(R, R') = \exp\left\{-\left(\frac{\Delta\tau}{2}\right)[E_L^{(k)}(R) + E_L^{(k)}(R')] + \Delta\tau E_T^{(k)}\right\}. \tag{9}$$

The $E_T^{(k)}$ are parameters that are changed during the simulation to keep $w^{(k)} \approx 1$ and the $E_L^{(k)} = H_k\Psi_G/\Psi_G$ are local energies that depend on the Hamiltonians $H_k$ mentioned at the begin of this section, $k \equiv \{2, 2ddd, V\}$.

So far the only difference that we have with the standard DMC method is that, instead of one weight, we have three weights attached to each walker. Moreover, each one of these weights is updated as usual in the DMC method. However, for efficiency, the number of walkers must fluctuate according to branching rules. These need to be slightly generalized, because we have more than one weight per walker. Let us consider the three specific situations that can emerge for a given walker: (a) all weights $w^{(k)}$ are greater than 2—in this case, the walker is duplicated and each of the copies will carry half of the initial weights; (b) at least one of the weights of the walker is in the range of a threshold value (which we have chosen to be 0.3) and 2—in this situation, it is kept with all its updated weights; (c) all weights are lower than the threshold value—in the last case, the walker will eventually be combined with another one in similar conditions if it is found in the present generation. For definiteness, let us suppose

that walkers $i$ and $j$ have all theirs weights below the threshold value. We compute the ratios $r^{(k)} = w_i^{(k)}/(w_i^{(k)} + w_j^{(k)})$ and assign the weight $w_i^{(k)} + w_j^{(k)}$ to configuration $i$ with probability $r^{(k)}$. If the value $w_i^{(k)} + w_j^{(k)}$ is not assigned to configuration $i$, it is ascribed to configuration $j$. Unless all the weights of a walker are zero, both walkers need to be kept. This is an undesirable situation, since walkers with one or more weights equal to zero erodes the correlation that we want to construct. Fortunately, the number of such walkers can be minimized with an adequate choice of the threshold value for the recombination of walkers. We have verified that, for a threshold value of 0.3, the number of walkers with one or more weights equal to zero is not greater than 5% of the total number of walkers. After the diffusion, weight update and branching, a so-called generation has been complete and the new set of walkers are ready for another diffusion step.

Periodically energy estimates of the system as weighted averages over the walkers using their corresponding local energies are recorded

$$E_k(R_i) = \frac{\sum_i w^{(k)}(R_i) E_L^{(k)}(R_i)}{\sum_i w^{(k)}(R_i)}. \tag{10}$$

The energy averages calculated in (10) with the different potentials are correlated, since they were computed using basically a single set of configurations. The contribution to the binding energy from the damped ATM potential $V_{ddd}$ can be computed without the need of extrapolation. It is a simple calculation performed by the subtraction

$$E_{ddd}(R_i) = E_{2ddd}(R_i) - E_2(R_i). \tag{11}$$

The analogous contribution from the exchange term $V_J$ is computed by

$$E_J(R_i) = E_V(R_i) - E_{2ddd}(R_i). \tag{12}$$

As usual, several generations have to be performed before we start accumulating the quantities of interest. After the system has been equilibrated, block averages of all the quantities of interest are formed and their estimated errors are computed.

In summary, the MW extension to the DMC method allows the determination of small energy differences like those of the three-body contributions to the total energy because they are computed using quantities obtained in a correlated form. Of course, the estimated values of $E_V$, $E_{2ddd}$ and $E_2$ within statistical uncertainties do not differ from values computed with the standard DMC method.

## 4. The simulations

In the liquid phase we chose a guiding function of the Jastrow form

$$\Psi_J(R) = \prod_{i<j} f(r_{ij}), \tag{13}$$

where $f(r_{ij}) = \exp(-u(r_{ij})/2)$ correlates a pair of particles with a pseudopotential of the McMillan form, $u(r_{ij}) = (b/|\mathbf{r_i} - \mathbf{r_j}|)^5$; $b$ is a parameter.

For the solid phase, a guiding function of the Nosanov–Jastrow form $\Psi_{NJ}(R) = \Phi_N(R)\Psi_J(R)$ was used:

$$\Phi_N(R) = \prod_i \exp\left[-\frac{C}{2}(\mathbf{r}_i - \mathbf{l}_i)^2\right], \tag{14}$$

where $\Phi_N$ represents a mean-field term that explicitly localizes the particles around given lattice sites $\mathbf{l}_i$. Explicit three-body correlation [14] could be included in the guiding function of both phases, with the advantages of faster convergence and small fluctuations, at a price of more evolved programming.

Although helium solidifies in a hexagonal close packed (hcp) structure, an fcc lattice was imposed in the simulations of the solid phase for computational convenience. The small energy differences [15] due to this approximation is within our statistical uncertainties in the calculations of the energies associated with the Hamiltonians $H_k$. All the results of the simulations were performed with 108 atoms in a cubic box with periodic boundary conditions. The pseudopotential of the correlation factor in (13) is slightly modified, $u(r) \rightarrow u(r) + u(L-r) - 2u(L/2)$, so that it goes smoothly to zero at half of the simulation cell, $L/2$. The size of the simulation box varies at each calculation and is computed by taking into account the number of particles ($N$) and density ($\rho$) considered in the simulation, i.e. $L = \sqrt[3]{N/\rho}$. The minimum image convention was used to calculate distances between a pair of particles in the simulation box. In the calculations of the three-body interactions we have slightly modified the minimum image convention [7] in order to compute the correct size of the third side of the triangles. At each density the averages of the quantities of interest were formed with about 500 estimates, each obtained after four time steps. Plots of energy versus time steps were used to assure that we have converged results. In all runs, the initial set of configurations are sampled from $|\Psi_{\{J,NJ\}}|^2$ using the Metropolis algorithm.

In principle, an extrapolation to $\Delta\tau \rightarrow 0$ has to be performed to compute the true quantities obtained in a calculation using the DMC method or in its MW extension. However, in our simulations we have chosen a time-step value such that more than 99% of the attempted moves are accepted. We have verified that, at this acceptance ratio, the extrapolation of the energies to $\Delta\tau \rightarrow 0$ agrees within statistical uncertainties with the values obtained directly from the simulation. Therefore we have kept such an acceptance ratio and disregard extrapolations.

We have considered tail corrections to compute the contributions of the two-body and $V_{ddd}$ potentials. The correction associated with the two-body potential at distances larger than half the side of the simulation cell was computed using the sum of one to three damped sinusoidal functions fitted to the computed pair radial distribution function $g_2(r)$. For the three-body part of the inter-atomic potential, the tail correction is computed by

$$T_3 = \frac{4\pi^2 N\rho^2}{3} \int_0^\infty \int_{L/2}^\infty \int_{-1}^1 g_3(r_{12}, r_{13}, r_{23}) V_{ddd}(r_{12}, r_{13}, r_{23}) \times r_{12}^2 r_{13}^2 \, \mathrm{d}x \, \mathrm{d}r_{12} \, \mathrm{d}r_{13}, \tag{15}$$

where $\rho$ is the density of the system, $r_{23}^2 = r_{12}^2 + r_{13}^2 - 2r_{12}r_{13}x$, and $x = \cos\theta$, where $\theta$ is the angle between $r_{12}$ and $r_{13}$. The Kirkwood superposition approximation, $g_3(r_{12}, r_{13}, r_{23}) \approx g_2(r_{12})g_2(r_{13})g_2(r_{23})$, was employed in (15). As in the calculation of the two-body tail correction, at distances large than half the side of the simulation box we have considered damped sinusoidal functions fitted to the pair correlation function $g_2(r)$. It is not difficult to realize by considering the limits of integration in (15) that all triangles outside the simulation cell were considered. No tail correction was performed for the exchange part of the inter-atomic potential due to the smallness of its contribution.

In the integration of the two- and three-body tail corrections, we have used Romberg's integration scheme with Richardson-style extrapolation. Since the mixed estimator, $\langle\Psi_G|O|\Psi\rangle$, for the expectation value of an operator $O$ only gives the exact result when it commutes with the Hamiltonian, the pair correlation function $g_2(r)$ was calculated using the linear extrapolation approximation $\langle\Psi|O|\Psi\rangle \approx 2\langle\Psi_G|O|\Psi\rangle - \langle\Psi_G|O|\Psi_G\rangle$, where $\langle\Psi_G|O|\Psi_G\rangle$ is the variational expectation value and $|\Psi\rangle$ is the exact ground state. We have estimated that for a system of 108 atoms in the liquid phase the tail correction due to the ATM three-body potential gives an additional contribution of about 6% to its computed value. In the solid phase, this value increases to approximately 8%. The contributions of the two- and three-

**Table 1.** Total energies per atom in units of K obtained in calculations using the $V$, $V_{2ddd}$ and $V_2$ potentials at the given densities. In the last column we show experimental data from [17] and [20] or values obtained from the Exp-EOS.

| $\rho$ (nm$^{-3}$) | $E_V$ | $E_{2ddd}$ | $E_2$ | Exp. |
|---|---|---|---|---|
| | | Liquid | | |
| 21.86 | $-7.171 \pm 0.008$ | $-7.195 \pm 0.008$ | $-7.316 \pm 0.008$ | $-7.170$[a] |
| 23.20 | $-7.120 \pm 0.008$ | $-7.148 \pm 0.008$ | $-7.288 \pm 0.008$ | $-7.114$ |
| 24.01 | $-7.020 \pm 0.008$ | $-7.050 \pm 0.008$ | $-7.202 \pm 0.008$ | $-7.027$[b] |
| 24.83 | $-6.897 \pm 0.009$ | $-6.929 \pm 0.009$ | $-7.096 \pm 0.009$ | $-6.893$ |
| 25.36 | $-6.778 \pm 0.009$ | $-6.812 \pm 0.009$ | $-6.987 \pm 0.009$ | $-6.782$ |
| 26.23 | $-6.544 \pm 0.009$ | $-6.579 \pm 0.009$ | $-6.770 \pm 0.009$ | — |
| | | Solid | | |
| 29.34 | $-5.780 \pm 0.009$ | $-5.780 \pm 0.009$ | $-6.035 \pm 0.009$ | $-5.789$[c] |
| 30.11 | $-5.550 \pm 0.009$ | $-5.548 \pm 0.009$ | $-5.821 \pm 0.009$ | $-5.56$ |
| 30.88 | $-5.277 \pm 0.009$ | $-5.271 \pm 0.009$ | $-5.562 \pm 0.009$ | $-5.28$ |
| 31.50 | $-5.016 \pm 0.009$ | $-5.005 \pm 0.009$ | $-5.310 \pm 0.009$ | $-5.021$[c] |
| 32.55 | $-4.509 \pm 0.009$ | $-4.491 \pm 0.009$ | $-4.822 \pm 0.009$ | $-4.50$ |
| 33.54 | $-3.938 \pm 0.009$ | $-3.909 \pm 0.009$ | $-4.265 \pm 0.009$ | $-3.919$[c] |
| 34.41 | $-3.312 \pm 0.009$ | $-3.271 \pm 0.009$ | $-3.652 \pm 0.009$ | $-3.32$ |
| 35.27 | $-2.690 \pm 0.009$ | $-2.640 \pm 0.009$ | $-3.043 \pm 0.009$ | $-2.681$[c] |

[a] Experimental value at 21.83 nm$^{-3}$.
[b] Interpolated value from [17].
[c] Interpolated value from [20].

body tail corrections, for the liquid and solid phases, were taken into account in the results presented in section 5.

## 5. Results

In the next two subsections we give details of the equations of state for both the liquid and solid phases of systems of $^4$He atoms obtained with all the Hamiltonians that we have considered in this work. These equations are importance by themselves, and also because some of the properties that we want to analyse depend on their analytical representations. Such analysis is made in the two last subsections.

Energies per atom in each phase as a function of the density $\rho$ were fitted to the expression

$$E(\rho) = E_0 + A\left(\frac{\rho - \rho_0}{\rho_0}\right)^2 + B\left(\frac{\rho - \rho_0}{\rho_0}\right)^3. \tag{16}$$

This depends on four parameters, $E_0$, $\rho_0$, $A$ and $B$. In the liquid phase the first two parameters have a physical signification on their own. The first one, $E_0$, represents the binding energy at the equilibrium density, and $\rho_0$ is the equilibrium density itself.

### *5.1. Equation of state for the liquid phase*

The liquid phase was investigated by considering systems of helium atoms at six densities ranging from 21.86 to 26.23 nm$^{-3}$. This range goes practically from the experimental equilibrium density, 21.83 nm$^{-3}$, to a value slightly above the experimental freezing density, 25.97 nm$^{-3}$ [16]. In table 1 we present the binding energies computed with the potentials $V_2$, $V_{2ddd}$ and $V$ together with experimental data [17] or values obtained through an analytical

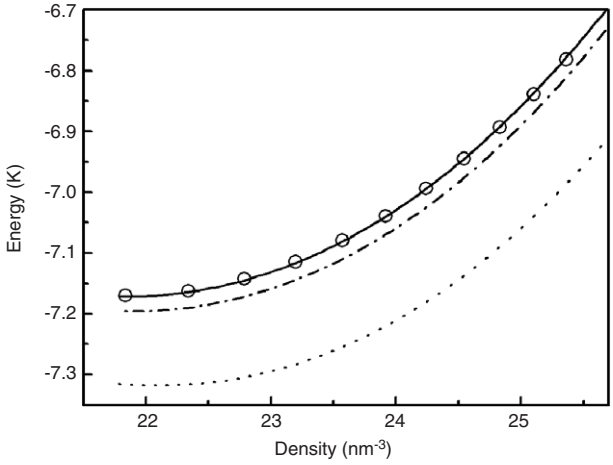


**Figure 1.** Equations of state for the liquid phase obtained using the $V_2$ (dotted line), $V_{2ddd}$ (dashed–dotted line), and $V$ (solid line) potentials. The circles represents experimental data from [17].

**Table 2.** Energies per atom in units of K associated with the damped ATM ($V_{ddd}$) and exchange ($V_J$) potentials at the given densities.

| $\rho$ (nm$^{-3}$) | $E_{ddd}$ | $E_J$ |
|---|---|---|
| | Liquid | |
| 21.86 | $0.121 \pm 0.001$ | $0.024 \pm 0.002$ |
| 23.20 | $0.140 \pm 0.001$ | $0.028 \pm 0.002$ |
| 24.01 | $0.152 \pm 0.001$ | $0.030 \pm 0.002$ |
| 24.83 | $0.167 \pm 0.001$ | $0.032 \pm 0.002$ |
| 25.36 | $0.175 \pm 0.001$ | $0.034 \pm 0.002$ |
| 26.23 | $0.191 \pm 0.001$ | $0.035 \pm 0.003$ |
| | Solid | |
| 29.34 | $0.255 \pm 0.001$ | $0.000 \pm 0.002$ |
| 30.11 | $0.273 \pm 0.001$ | $-0.002 \pm 0.002$ |
| 30.88 | $0.291 \pm 0.001$ | $-0.006 \pm 0.002$ |
| 31.50 | $0.305 \pm 0.001$ | $-0.011 \pm 0.002$ |
| 32.55 | $0.331 \pm 0.001$ | $-0.018 \pm 0.002$ |
| 33.54 | $0.356 \pm 0.001$ | $-0.029 \pm 0.002$ |
| 34.41 | $0.381 \pm 0.001$ | $-0.041 \pm 0.002$ |
| 35.27 | $0.403 \pm 0.001$ | $-0.050 \pm 0.002$ |

equation of state (EOS) fitted to the experimental data (Exp-EOS). Analytical equations of state fitted to these results are compared with experimental binding energies [17] in figure 1. As we can see, the theoretical results obtained with the inter-atomic potential $V$ are in excellent agreement with the experimental values at all densities. Although the results obtained in calculations using the $V_{2ddd}$ potential are much closer to experiment than those where only the two-body potential $V_2$ is employed, still in most cases these results fail to be in agreement with experiment. The EOS for the various potentials shows in a clear way how the results evolve when $V_{ddd}$ and $V_J$ are included in the interacting potential. The fitting parameters of the EOS for all the potentials and the Exp-EOS are presented in table 3.

In the liquid phase the three-body potentials $V_{ddd}$ and $V_J$ give positive contributions to the total energy, as we can see in table 2. As we go from the lowest density to the highest

**Table 3.** Fitting parameters for the equations of state in the liquid and solid phases, obtained with results of the given potentials. Exp-EOS denotes the fitting parameters determined using experimental binding energies. In the last line, for the liquid phase, we present published experimental values of the given quantities.

| Potential | $\rho_0$ (nm$^{-3}$) | $E_0$ (K) | $A$ (K) | $B$ (K) |
|---|---|---|---|---|
| | | Liquid | | |
| $V_2$ | $22.10 \pm 0.13$ | $-7.318 \pm 0.004$ | $13.5 \pm 1.7$ | $11.6 \pm 4.3$ |
| $V_{2ddd}$ | $21.87 \pm 0.14$ | $-7.196 \pm 0.004$ | $13.4 \pm 1.8$ | $10.6 \pm 3.8$ |
| $V$ | $21.82 \pm 0.14$ | $-7.172 \pm 0.004$ | $13.3 \pm 1.8$ | $10.0 \pm 3.8$ |
| $V_{\rm pr3}$[a] | $21.80 \pm 0.02$ | $-7.178 \pm 0.002$ | | |
| $V_{\rm HF3}$[a] | $21.68 \pm 0.02$ | $-7.124 \pm 0.002$ | | |
| Exp-EOS[b] | $21.820 \pm 0.004$ | $-7.1701 \pm 0.0001$ | $13.449 \pm 0.086$ | $7.82 \pm 0.30$ |
| Exp. | 21.834[c] | $-7.170$[d] | | |
| | | Solid | | |
| $V_2$ | $26.40 \pm 0.08$ | $-6.377 \pm 0.011$ | $26.8 \pm 1.4$ | $8.2 \pm 2.0$ |
| $V_{2ddd}$ | $26.14 \pm 0.09$ | $-6.187 \pm 0.013$ | $26.3 \pm 1.4$ | $8.1 \pm 1.9$ |
| $V$ | $25.98 \pm 0.10$ | $-6.202 \pm 0.014$ | $24.2 \pm 1.5$ | $9.3 \pm 1.8$ |
| Exp-EOS[e] | $26.02 \pm 0.70$ | $-6.220 \pm 0.097$ | $25.6 \pm 7.7$ | $6.8 \pm 7.3$ |

[a] Reference [8].
[b] Fitting parameters using data of [17].
[c] Reference [16].
[d] Reference [17].
[e] Fitting parameters using data of [20].

density, the contribution associated with the damped ATM term to the binding energy goes from approximately 2 to 3% of the modulus of $E_V$, the binding energy computed using the potential $V$. In a similar comparison, the contribution of the exchange term goes from about 0.3 to 0.5%. In particular, its contribution is about 18% of the triple–dipole dispersion energy at our highest density. Despite the smallness of the energy associated with the exchange term in the inter-atomic potential, its importance is remarkable. It just cannot be neglected if very accurate results are needed [2].

In order to verify the importance of the phenomenological parameters $\mathcal{A}$ and $\delta_d$ in the three-body inter-atomic potential, it is necessary to compare the results of this work with others previously published in which different inter-atomic potentials were used. These results are shown in table 4. All the inter-atomic potentials presented in table 4 used as the three-body part of the interaction the potential of Cohen and Murrell [6], i.e. $V_J$ and $V_{ddd}$ with parameter values $\mathcal{A} = 1.0$ and $\delta_d = 0$, respectively. The two-body part used by the inter-atomic potentials of table 4 are: for the potential $V_{003}$, the two-body interaction proposed by Hurley and Moldover [18]; for the potential $V_{\rm HF3}$, the two-body interaction proposed by Aziz *et al* [19]; finally, in the inter-atomic potential $V_{\rm pr3}$, the two-body potential of (2) was used. Note that the only difference between the potentials $V$ and $V_{\rm pr3}$ are the values of the phenomenological parameters used.

We see from table 4 that a good agreement between theory and experiment was achieved when we used the potentials $V_{\rm pr3}$ and $V_{003}$ to describe the equation of state in the liquid phase. The potential $V_{\rm HF3}$ was incapable of reproducing the experimental binding energies of this phase. Note that, although it was possible to reproduce the equation of state of the liquid phase with the inter-atomic potentials $V_{\rm pr3}$ and $V_{003}$ (with these results the use of phenomenological parameters in $V_J$ and $V_{ddd}$ will not be justified), they fail when we try to describe the equation of state in the solid phase, as we show in the next section.

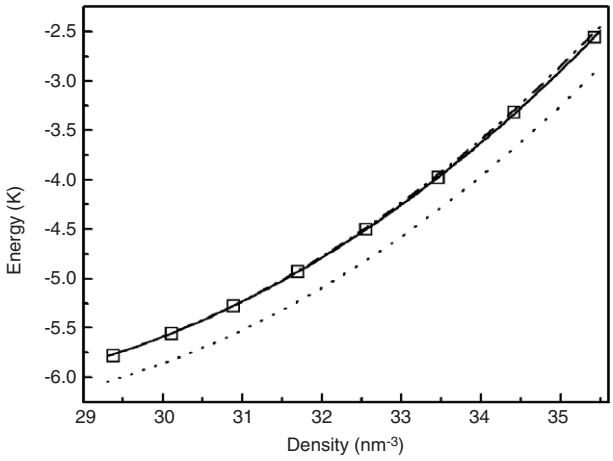


**Figure 2.** Equations of state for the solid phase determined using the $V_2$ (dotted line), $V_{2ddd}$ (dashed–dotted line), and $V$ (solid line) potentials. The squares represent experimental data from [20]. Due to the figure scale, in some regions the EOS obtained using the $V_{2ddd}$ and the $V$ potentials cannot be distinguished.

**Table 4.** Total energies per atom in units of K obtained in calculations using the $V_{003}$, $V_{\rm pr3}$ and $V_{\rm HF3}$ potentials [8] at the given densities.

| $\rho$ (nm$^{-3}$) | $E_{003}$ | $E_{\rm pr3}$ | $E_{\rm HF3}$ |
|---|---|---|---|
| | | Liquid | |
| 21.86 | $-7.190 \pm 0.008$ | $-7.174 \pm 0.008$ | $-7.120 \pm 0.008$ |
| 23.20 | — | $-7.128 \pm 0.009$ | $-7.062 \pm 0.009$ |
| 24.01 | — | $-7.029 \pm 0.009$ | $-6.956 \pm 0.009$ |
| 24.83 | $-6.903 \pm 0.010$ | $-6.885 \pm 0.010$ | $-6.805 \pm 0.010$ |
| 25.33 | — | $-6.780 \pm 0.011$ | $-6.694 \pm 0.011$ |
| 26.23 | $-6.551 \pm 0.011$ | $-6.532 \pm 0.011$ | $-6.437 \pm 0.011$ |
| | | Solid | |
| 29.34 | $-5.748 \pm 0.009$ | $-5.725 \pm 0.009$ | $-5.625 \pm 0.009$ |
| 30.11 | — | $-5.497 \pm 0.009$ | $-5.390 \pm 0.009$ |
| 31.50 | $-4.972 \pm 0.009$ | $-4.948 \pm 0.009$ | $-4.825 \pm 0.009$ |
| 32.88 | — | $-4.231 \pm 0.009$ | $-4.085 \pm 0.009$ |
| 33.54 | $-3.854 \pm 0.009$ | $-3.830 \pm 0.009$ | $-3.675 \pm 0.009$ |
| 34.41 | — | $-3.207 \pm 0.010$ | $-3.040 \pm 0.010$ |
| 35.27 | $-2.562 \pm 0.010$ | $-2.537 \pm 0.010$ | $-2.352 \pm 0.010$ |

### *5.2. Equation of state for the solid phase*

The equations of state for the solid phase were investigated by employing the potentials $V_2$, $V_{2ddd}$ and $V$ at eight densities. They lie in a range where accurate experimental data are available. The lowest density that we have considered, 29.34 nm$^{-3}$, is slightly higher than the experimental [20] melting density, 28.57 nm$^{-3}$. In figure 2 we compare the fitted equations of state to results obtained with the three potentials to experimental binding energies [20]. The values from theory and experiment are displayed in table 1. As we may see, the EOS determined using the inter-atomic potential $V$ gives binding energies that are in excellent agreement with the experimental data at all the densities. We can also see that at the high

end of the density range the energies computed with the potential $V_{2ddd}$ are too high. This is a situation that the inclusion of the exchange potential $V_J$ in the inter-atomic potential is able to correct. The fitting parameters of the analytical equations of state for both theoretical results and for the experimental data for the solid phase are presented in table 3.

In the solid phase the damped ATM interaction gives a positive contribution to the system energy. The exchange term at the density 30.88 $nm^{-3}$ and above certainly gives a negative contribution to the total energy. Results associated with the ATM and exchange terms for this phase are presented in table 2. As we go from the lowest density to the highest density, the contribution of the ATM term to the total energy goes approximately from 4 to 15% of the modulus of $E_V$. At the beginning of the density range the exchange term practically does not give any contribution to the total energy. At the end of this interval it lowers $E_V$ by about 2%. In more details, the three-body exchange energy at our highest density is attractive and its modulus is about 12% of the dispersion energy. The contribution of both the triple–dipole and the exchange potentials to the binding energy are more important in this phase.

As performed in the previous section, it is necessary to compare the results obtained in this work for the solid phase with those obtained using the inter-atomic potentials of table 4. We see from table 4 that none of the potentials that we previously used, $V_{pr3}$, $V_{003}$ and $V_{HF3}$, were able to reproduce the equation of state of the solid phase. The differences that we found between the experimental binding energies and the energies obtained with the potentials $V_{pr3}$ and $V_{003}$ go from ≈0, 050 K, at the lowest density studied, to ≈0, 130 K at the highest density studied. The difference is still greater when we compare the results obtained with the potential $V_{HF3}$. In this case we found, going from the lowest density to the highest density, a difference of ≈0, 120 to ≈0, 320 K, respectively. In other words, the potentials $V_{pr3}$, $V_{003}$ and $V_{HF3}$ were incapable of describing correctly and simultaneously the liquid and solid phases of helium atoms. It is the potential $V$ in (1), with the parameter values $\delta_d = 20.352$ $nm^{-1}$ and $\mathcal{A} = 4.0$, that gives a good description of the condensed phases of the helium atoms systems.

### *5.3. Equilibrium, melting and freezing densities*

The value of the equilibrium density $\rho_0$ calculated from the fits of equations of state to the results determined using the potentials $V_2$, $V_{2ddd}$ and $V$ are presented in table 3. As we can see, the equilibrium density evolves towards the experimental value as the potential in the calculations is refined. The most important contribution from the three-body interactions to this quantity comes from the damped ATM term. The equilibrium density determined with the inter-atomic potential $V$, $21.82 \pm 0.14$ $nm^{-3}$, is in excellent agreement with the experimental value of 21.834 $nm^{-3}$ and the value obtained from the Exp-EOS. We stress that, since all of our results are correlated, the changes reported in $\rho_0$ are significant, despite the statistical fluctuations that each value may have.

The melting and freezing densities were calculated from the Maxwell double tangent construction using the analytical equations of state for the liquid and solid phases. The computed values for all the potentials that we have considered are presented in table 5. The value of the freezing density computed using the $V_{2ddd}$ potential is worse than the one obtained through the two-body potential $V_2$. The freezing and melting density values determined using the inter-atomic potential $V$ put in evidence the importance of the exchange contribution to the inter-atomic potential. These last results are the closest to the values from experiment. Note that all potentials produce results that are in agreement with the experimental values. However, since these quantities are computed using basically a single set of walkers, it is simple to follow how they change as three-body terms are included in the interacting potential.

**Table 5.** The melting, $\rho_m$, and freezing, $\rho_f$, densities in $nm^{-3}$ for the given potentials and experiment. In the last two lines we present published experimental values.

| Potential | $\rho_m$ | $\rho_f$ |
|---|---|---|
| $V_2$ | $29.07 \pm 0.32$ | $26.05 \pm 0.32$ |
| $V_{2ddd}$ | $29.04 \pm 0.31$ | $26.09 \pm 0.31$ |
| $V$ | $28.93 \pm 0.31$ | $25.95 \pm 0.31$ |
| $V_{\rm pr3}$[a] | $28.98 \pm 0.18$ | $25.98 \pm 0.18$ |
| $V_{\rm HF3}$[a] | $28.91 \pm 0.22$ | $25.90 \pm 0.21$ |
| Exp-EOS | $28.88 \pm 0.43$ | $26.02 \pm 0.40$ |
| [16] | — | $25.970 \pm 0.005$ |
| [20] | 28.568 | — |

[a] Reference [8].

In tables 3 and 5 we show results for the equilibrium, freezing and melting densities obtained with the potentials $V_{\rm pr3}$ and $V_{\rm HF3}$. We see from this table that it is possible to employ the inter-atomic potential $V_{\rm pr3}$ to calculate the equilibrium, melting and freezing densities with good results. This is not the case for the potential $V_{\rm HF3}$, which fails to describe the equilibrium density. Since the results for the freezing and melting densities using the potentials $V$ and $V_{\rm pr3}$ are similar (see table 5), we can affirm that the equations of state are roughly equally displaced from each other at the regions of high-density liquids and low-density solids when we include our phenomenological parameters in $V$. Also, looking to the equilibrium density results of table 3, we can conclude that the minimum of the equation of state is almost unaffected by the inclusion of these parameters.

### *5.4. Pressure, isothermal compressibility and sound velocity*

The pressure $P$

$$P(\rho) = \rho^2 \left( \frac{\partial E}{\partial \rho} \right), \tag{17}$$

the isothermal compressibility

$$K(\rho) = \frac{1}{\rho} \left[ \frac{\partial \rho}{\partial P} \right]_T, \tag{18}$$

and the sound velocity

$$c(\rho) = \left[ \frac{1}{mK\rho} \right]^{1/2}, \tag{19}$$

have been computed in the liquid phase using results from all three Hamiltonians that we have considered in this work. In table 6 we show the results for these three quantities evaluated at the experimental equilibrium density. We have chosen to evaluate these quantities at the experimental value of the equilibrium density in order to make clearer how the results evolve with the different potentials.

The computed values of the pressure in table 6 are very sensitive to both the equilibrium density $\rho_0$ value and the curvature of the EOS. Evidence of this behaviour is the difference of about 1 atm found between the results obtained with the $V_2$ and $V$ potentials. The damped ATM term accounts for approximately 80% of the observed increase in the value of this quantity towards zero, its true value. The remaining increase of 20% is due to the exchange term. This is not a small amount and it appears despite the small contribution of this term in the binding energy of the liquid phase.

**Table 6.** Values for the pressure $P$ (atm), isothermal compressibility $K$ ($atm^{-1}$) and sound velocity $c$ ($m\ s^{-1}$) calculated with the given potentials at the experimental equilibrium density, 21.834 $nm^{-3}$. In the last line the isothermal compressibility was obtained through (19) using the experimental data of [16].

| Potential | $P$ | $K$ | $c$ |
|---|---|---|---|
| $V_2$ | $-0.94 \pm 0.19$ | $0.0135 \pm 0.0006$ | $227.53 \pm 0.76$ |
| $V_{2ddd}$ | $-0.12 \pm 0.18$ | $0.0127 \pm 0.0005$ | $234.39 \pm 0.74$ |
| $V$ | $0.05 \pm 0.18$ | $0.0126 \pm 0.0005$ | $235.79 \pm 0.74$ |
| $V_{\mathrm{pr3}}$[a] | $0.11 \pm 0.06$ | $0.0126 \pm 0.0002$ | $235.86 \pm 0.45$ |
| Exp-EOS | $0.051 \pm 0.017$ | $0.01245 \pm 0.000\,08$ | $236.81 \pm 0.23$ |
| Exp | — | 0.0123 | 238.30[b] |

[a] Reference [8].
[b] Reference [21].

The isothermal compressibility result obtained with the $V$ potential is in excellent agreement, within statistical fluctuations, with the experimental value and the value obtained using the Exp-EOS. The damped ATM and exchange three-body interactions lower the computed isothermal compressibility, improving agreement with experiment. Mainly because of the ATM term, the computed value of this quantity decreases by about 7% when we compare results obtained with the $V_2$ and $V$ potentials.

The sound velocity computed using the $V$ potential and the Exp-EOS are in agreement. However, neither of them agree with the accepted experimental value, 238.30 $m\ s^{-1}$ [21]. It seems that this quantity cannot be computed in a satisfactory way by considering the equations of state together with (17)–(19).

We can see from table 6 that similar descriptions of the pressure, isothermal compressibility and sound velocity can be achieved using the inter-atomic potentials $V$ and $V_{\mathrm{pr3}}$. We can conclude, comparing both results, that the inclusion of the phenomenological parameters in the three-body part on the inter-atomic potential $V$ do not modify the concavity of the liquid equation of state. The main roll of these parameters is to modulate the intensity of the three-body contributions without altering the shape of the equation of state.

## 6. Final comments

In this work we have investigated in detail how small energy contributions from three-body terms of the inter-atomic potential $V$ modify many properties of a system of $^4$He atoms and contribute to its total energy. We have computed the energies associated with the triple–dipole and exchange potentials at several densities of the liquid and solid phases. These results have confirmed [2] both that $V_{ddd}$, the ATM term, is the dominant three-body interaction and that the exchange component $V_J$ cannot be neglected in the inter-atomic potential $V$.

The importance of the small exchange term $V_J$ in the potential it is not limited to the energy of the system. In the liquid phase, quantities like the isothermal compressibility and the equilibrium density itself have their agreement with experiment enhanced as we include the potentials $V_{ddd}$ and $V_J$ in the interaction between the atoms. We can draw these conclusions despite the fact that the values of the above quantities are computed with uncertainties much larger than the observed change in their values. This is because we have performed the calculations using the MW extension to the DMC method which correlates the results.

A more stringent test of how the three-body terms of the inter-atomic potential affect the system might be obtained from the calculations of the melting and freezing densities which depend on the description of the system in both the solid and liquid phases. Our results for

these quantities in table 5 show evidence that the potential $V$ is more than just a piling up of three-body terms into the two-body potential $V_2$. The freezing density steadily decreases to the experimental value as the $V_{ddd}$ and the $V_J$ are included. However, the melting density first gets worse and then gets closer to the experimental value. It is the full inter-atomic potential $V$ that gives the most accurate description of the systems of helium atoms. Just part of it can be even worse than the result of a simpler potential.

Although very good results can be obtained in the description of many properties of systems of helium atoms using the inter-atomic potential $V$ that includes the three-body terms $V_{ddd}$ and $V_J$, some questions remain. First, the amplitude of $V_J$ is four times larger than the amplitude determined by *ab initio* calculations [6] for trimers. In this context is important to mention that we were not able to reproduce the published values in [6] (we obtained only close results) using the parameters given within the article. Although the differences found between the published values and the obtained values are not huge, a doubt arises concerning the precision of the parameters in [6]. However, these differences do not justify the great increase (from 1.0 to 4.0) of our phenomenological parameter $\mathcal{A}$ in $V_J$. Second, the multi-polar non-additive third-order contributions to the dispersion energy are assumed to cancel the fourth- and higher-order dipole interaction terms. This is true, most probably, only approximately. In other words, we have an inter-atomic potential that is able to give a very good description of the systems of helium atoms in the condensed phases. However, a reasonable understanding of its three-body and high-order contributions is still lacking. We hope that our work will contribute to prompting further efforts to clarify these issues.

## Acknowledgments

This work was conducted, in part, using the facilities of the 'Centro Nacional de Processamento de Alto Desempenho em São Paulo'. Sebastian Ujevic acknowledges financial support from 'Financiadora de Estudos e Projetos—FINEP' and 'Ministério da Ciência e Tecnologia—MCT'. S A Vitiello acknowledges financial support from 'Fundação de Amparo à Pesquisa do Estado de São Paulo—FAPESP'.

## Appendix A. Parameters of the $V_2$ potential and its retardation function $\phi_{\mathcal{R}}$

**Table A.1.** Parameter values of the $V_2$ potential, Korona *et al* [9].

| Parameter | Value | Parameter | Value (au) |
|---|---|---|---|
| $A$ | 2074 364.26 K | $C_8$ | 14.117 855 |
| $\alpha$ | 1.886 482 51 bohr$^{-1}$ | $C_{10}$ | 183.691 25 |
| $\beta$ | −0.062 001 3490 bohr$^{-2}$ | $C_{12}$ | 3265 |
| $\delta$ | 1.948 612 95 bohr$^{-1}$ | $C_{14}$ | 76 440 |
| $C_6$ | 1.460 9778 (au) | $C_{16}$ | 2275 000 |

**Table A.2.** Retardation function $\phi_{\mathcal{R}}(r)$ of the $V_2$ potential, [3].

| Range (bohr) | $\phi_{\mathcal{R}}(r)$ |
|---|---|
| $0 \leqslant r < 5.7$ | 1 |
| $5.7 \leqslant r < 10$ | $p_1 + p_2 r + p_3 r^2 + p_4 r^3$ |
| $10 \leqslant r < 10^2$ | $1 - p_1 - p_2 r^{0.5} - p_3 r - p_4 r^{1.5} - p_5 r^2$ |
| $10^2 \leqslant r < 2 \times 10^2$ | $(1 + p_1 + p_2 r^{0.5} + p_3 r + p_4 r^2)/(1.2 + 0.8 p_5 r)$ |
| $2 \times 10^2 \leqslant r < 10^3$ | $\ln(r(p_1 r^{0.4} + p_2 r^{0.5} + p_3 r^{0.6} + p_4 r^{0.7} + p_5 r^{0.8}))$ |
| $10^3 \leqslant r < 10^4$ | $p_1 + p_2 r^{-1} + p_3 r^{-2} + p_4 r^{-3} + p_5 r^{-4}$ |
| $10^4 \leqslant r < 10^5$ | $p_1 + p_2 r^{-1} + p_3 r^{-2} + p_4 r^{-3} + p_5 r^{-4}$ |

**Table A.3.** Parameter values for the retardation functions $\phi_{\mathcal{R}}(r)$, [3].

| Range (bohr) | $p_1$ (au) | $p_2$ (au) | $p_3$ (au) |
|---|---|---|---|
| $5.7 \leqslant r < 10$ | $9.860\,029 \times 10^{-1}$ | $5.942\,027 \times 10^{-3}$ | $-7.924\,833 \times 10^{-4}$ |
| $10 \leqslant r < 10^2$ | $-1.623\,43 \times 10^{-3}$ | $2.220\,97 \times 10^{-3}$ | $-1.173\,23 \times 10^{-3}$ |
| $10^2 \leqslant r < 2 \times 10^2$ | $8.825\,06 \times 10^{-2}$ | $3.818\,46 \times 10^{-2}$ | $-1.724\,21 \times 10^{-3}$ |
| $2 \times 10^2 \leqslant r < 10^3$ | 1.488 897 | −2.123 572 | 1.043 994 |
| $10^3 \leqslant r < 10^4$ | $6.184\,108 \times 10^{-6}$ | $3.283\,043 \times 10^{2}$ | $1.367\,922 \times 10^{3}$ |
| $10^4 \leqslant r < 10^5$ | $-1.107\,002 \times 10^{-7}$ | $3.284\,717 \times 10^{2}$ | $-9.819\,846 \times 10^{2}$ |
| Range (bohr) | $p_4$ (au) | $p_5$ (au) | |
| $5.7 \leqslant r < 10$ | $3.172\,548 \times 10^{-5}$ | — | |
| $10 \leqslant r < 10^2$ | $3.000\,12 \times 10^{-4}$ | $-1.055\,12 \times 10^{-5}$ | |
| $10^2 \leqslant r < 2 \times 10^2$ | $4.748\,97 \times 10^{-7}$ | $3.044\,5706 \times 10^{-3}$ | |
| $2 \times 10^2 \leqslant r < 10^3$ | $-1.898\,459 \times 10^{-1}$ | $6.479\,867 \times 10^{-3}$ | |
| $10^3 \leqslant r < 10^4$ | $-4.464\,489 \times 10^{7}$ | $1.365\,003 \times 10^{10}$ | |
| $10^4 \leqslant r < 10^5$ | $-1.953\,816 \times 10^{7}$ | $-1.079\,712 \times 10^{11}$ | |

## Appendix B. Parameters of the exchange potential $V_J$

**Table B.1.** Parameter values for the exchange potential [6].

| Parameter[a] | Value | Parameter | Value |
|---|---|---|---|
| $\alpha$ | 3.446 Å$^{-1}$ | $c_7$ | −1726.015 |
| $c_0$ | −1957.895 | $c_8$ | 177.661 |
| $c_1$ | 673.186 | $c_9$ | 2693.277 |
| $c_2$ | −188.491 | $c_{10}$ | −1096.591 |
| $c_3$ | 3664.836 | $c_{11}$ | 154.063 |
| $c_4$ | −1655.476 | $c_{12}$ | 6011.520 |
| $c_5$ | 244.090 | $c_{13}$ | −2618.297 |
| $c_6$ | 4129.947 | $c_{14}$ | 296.384 |

[a] The parameters $c_i$ are in the appropriate units, i.e. $c_0 = eV_h$, $c_1 = eV_h$ Å$^{-1}$, etc; $1eV_h = 0.036726E_h$.

## References


[1] Whitlock P A and Vitiello S A 2006 *Lect. Notes Comput. Sci.* **3743** 40
[2] Ujevic S and Vitiello S A 2006 *Phys. Rev.* B **73** 012511
[3] Janzen A R and Aziz R A 1997 *J. Chem. Phys.* **107** 914
[4] Axilrod B M and Teller E 1943 *J. Chem. Phys.* **11** 299
[5] Muto Y 1943 *Proc. Phys. Math. Soc. Japan* **17** 629
[6] Cohen M J and Murrell J N 1996 *Chem. Phys. Lett.* **260** 371
[7] Ujevic S and Vitiello S A 2003 *J. Chem. Phys.* **119** 8482
[8] Ujevic S and Vitiello S A 2005 *Phys. Rev.* B **71** 224518
[9] Korona T, Williams H L, Bukowski R, Jeziorski B and Szalewicz K 1997 *J. Chem. Phys.* **106** 5109
[10] Tang K T and Toennies J P 1984 *J. Chem. Phys.* **80** 3726
[11] Etters R D and Danilowicz R 1979 *J. Chem. Phys.* **71** 4767
[12] Reynolds P J, Ceperley D M, Alder B J and Lester W A 1982 *J. Chem. Phys.* **77** 5593
[13] Umringar C J, Nightingale M P and Runge K J 1993 *J. Chem. Phys.* **99** 2865
[14] Vitiello S A and Schmidt K E 1999 *Phys. Rev.* B **60** 12342 and references therein
[15] Vitiello S A 2002 *Phys. Rev.* B **65** 214516

[16] Berthold J E, Hanson H N, Maris H J and Seidel G M 1976 *Phys. Rev.* B **14** 1902
[17] de Bruyn Ouboter R and Yang C N 1987 *Physica* B **144** 127
[18] Hurly J J and Moldover M R 2000 *J. Res. Natl Inst. Stand. Technol.* **105** 667
[19] Aziz R A, Janzen A R and Moldover M R 1995 *Phys. Rev. Lett.* **74** 1586
[20] Edwards D O and Pandorf R C 1965 *Phys. Rev.* A **140** 816
[21] Abraham B M, Eckstein Y, Ketterson J B, Kuchnir M and Roach P R 1970 *Phys. Rev.* A **1** 250